Sound Radiation by a Cylindrical Open Cavity with a Surface Source at the Bottom

Krzysztof SZEMELA

Department of Mechatronics and Control Science
University of Rzeszów
Pigonia 1, 35-310 Rzeszów, Poland; e-mail: alpha@ur.edu.pl

The rigorous solution describing the sound radiation by an arbitrary surface source located at the bottom of a cylindrical open cavity embedded in a flat baffle has been obtained. The open cavities of different shapes can be found in some architectural structures as well as are components of sensors, musical instruments and vehicles. The presented formulas have been expressed in the form of infinite sums. To use them, the infinite sums have to be truncated to the finite number of terms. Therefore, in practice, the results obtain based on the proposed solution are not exact and their accuracy is determined by the truncation error. The use of presented formulas is an alternative method for the finite element method (FEM). However, taking into account that the calculation efficiency of FEM rapidly decrease when a volume of considered region increases, the obtained in this study solution can be more useful in some practical cases.

The approximated formula of a high computational efficiency has been presented for the sound pressure in the far field. The sound radiation has been analyzed for a rectangular piston as a sound source. The influence of cavity depth ratio on the radiation efficiency has been investigated. The cases for which the cavity radiation efficiency can be approximately calculated from the formula valid for a baffled sound source have been determined.

Keywords: open cylindrical cavity; sound pressure; sound power; continuity conditions.

1. Introduction

At present, in an urban environment, the acoustic properties of objects which can generate some acoustic waves play an important role. For existing real vibroacoustic systems, the active vibration control methods have been proposed to modify structures vibrations and consequently their acoustic radiation. These methods have been developed for plates, device casings as well as more complicated objects (WICIAK, TROJANOWSKI, 2015; LENIOWSKA, MAZAN, 2015; JEONG et al., 2016; MAZUR, PAWEŁCZYK, 2016; WRONA, PAWEŁCZYK, 2016; PRAKASH et al., 2016).

In the case of designed objects, the theoretical investigations are used to predict and optimized their acoustic properties at the stage of construction. However, to use this methodology, the theoretical formulas are necessary. Therefore, there are a number of studies which provide some theoretical models, formulations as well as numerical methods which can be ap-

plied to analyze an acoustic behavior of different objects. The sound radiation of surface sources such as plates has often been examined based on theoretical models and mathematical methods (RDZANEK, 2016; UNRUH et al., 2015; CHOI et al., 2014; ZAWIESKA, RDZANEK, 2007). In practice, some radiators are often located inside regions such as, for example, acoustic rooms, waveguides, canyons as well as cavities. Acoustic waves generated in these cases interact with the regions walls which considerably change the acoustic radiation. Hence, the theoretical analysis performed for such vibroacoustic systems has to take into account some interference effects which makes it more complicated. Based on advanced mathematical methods and numerical techniques, the solutions describing the sound radiation have been presented for the acoustic rooms and waveguides (MEISSNER, 2013; BHUDDI et al., 2015; KARBAN et al., 2016; JURKIEWICZ et al., 2011; SNAKOWSKA et al., 2017). Additionally, the diffraction effect at the opening of a soft cylindrical

duct has been investigated (SNAKOWSKA, 2008). The acoustic behavior of different acoustic canyons has also been discussed (PELAT *et al.*, 2009; SZEMELA, 2015; LEE, KANG, 2015).

Some problems related to the acoustic radiation by cavities have been solved and discussed. The optimization of cavity shape taking into account its acoustic properties has been presented (TROIAN *et al.*, 2016). The acoustic resonance frequencies of the 2D and 3D open cavity have been determinated (GONZÁLEZ *et al.*, 2013; ORTIZ *et al.*, 2016). Making use of the statistical energy analysis, the interior noise of elongated cavity has been analyzed (YANG, CHENG, 2016). The acoustic behavior of cavities coupled with plates has been discussed. The time variation of vibroacoustic response has been examined for the system cavity – plate in the case when the plate is subjected to an arbitrary transient external excitation (HASHEMINEJAD *et al.*, 2012). The rigorous formulas describing the sound radiation of cylindrical cavity with a circular plate embedded at its opening and two pistons located inside have been obtained (RDZANEK *et al.*, 2016).

From a practical standpoint, some open cavities are interesting vibroacoustic systems. They can be found in some architectural structures as well as are components of sensors, musical instruments and vehicles. Moreover, outlets of different devices and machines can be considered as open cavities. Hence, there are many objects which acoustic properties can be determined based on the open cavity model.

The sound radiation by cavities can be solved with the use of the finite element method (FEM). However, an accuracy of this method is strongly influenced by an elements size used for FEM calculations. Moreover, the calculation efficiency of FEM rapidly decrease when a volume of considered region increases. Therefore, the mathematical formulas describing acoustic behavior of considered objects are useful in many practical cases as an alternative solution for FEM.

Making use of the modal decomposition and the continuity conditions, the theoretical analysis of the sound radiation has been performed in the case of the rigid-walled open rectangular cavity with a sound source located at its bottom (SZEMELA, 2017). The formulas for the sound pressure inside and outside cavity as well as for the sound power have been obtained. The influence of the vibration frequency and the sound source location on the acoustic behavior of the considered vibroacoustic system has been investigated. The presented results show some acoustic properties of open cavities with a sound source located at the bottom. However, to better know the acoustic behavior of open cavities, the analysis of sound radiation should also be performed for cavities of other shapes. Moreover, it is of practical importance to investigate the influence of the cavity depth on its acoustic radiation.

So far, the rigorous formulas for the sound pressure and sound power which can be used instead of the finite element method in the case of the cylindrical rigid-walled cavity with an arbitrary surface sound source located at the bottom have not been presented in the literature. Therefore, this study is focused on obtaining these formulations based on the modal decomposition and the continuity conditions. Additionally, the influence of cavity depth ratio on the radiation efficiency has been investigated. Moreover, the cases in which the cavity radiation efficiency can be approximately calculated from a less complicated formula valid for a baffled sound source have been determined. This can be used to improve the numerical calculations for shallow cavities.

2. Statement of the problem

A cylindrical open cavity with rigid walls and an opening embedded in a flat rigid and infinite baffle is considered. Acoustic waves propagate inside the two connected regions: the cavity interior is the region I and the half space above cavity is the region II. The cavity radius and depth are equal to a and H, respectively. It has been assumed that acoustic waves are generated by an arbitrary surface sound source located at the cavity bottom. To describe the sound radiation, the cylindrical coordinate system (r, φ, z) with the origin at the central point of the cavity bottom has been used (see Fig. 1). Additionally, the Cartesian coordinate system of the same origin has been introduced. The analysis has been performed for the steady-state and time-harmonic processes of the time dependence given by the following function $\exp(-i\omega t)$ where $\omega = 2\pi f$ is the vibration angular frequency, f is the vibration frequency and i is the imaginary unit. Moreover, it has been assumed that the same lossless, isotropic, homogeneous medium of the density ρ and with the sound speed c is inside as well as outside the cavity. Only acoustic waves of small amplitude have been analyzed. Hence, according to the acoustic field linear theory, the sound pressure inside and outside the cavity satisfies the following Helmholtz equation

$$\left(\nabla^2 + k^2\right) p_\beta(r, \varphi, z) = 0, \qquad \beta = 1, \, 2, \qquad (1)$$

where $\nabla^2 = \partial^2/\partial r^2 + (1/r)\partial/\partial r + (1/r^2)\partial^2/\partial\varphi^2 + \partial^2/\partial z^2$, $k = \omega/c$ is the wave number, $p_1(r, \varphi, z)$ and $p_2(r, \varphi, z)$ are the sound pressure for the region I and II, respectively. Moreover, at the cavity opening, the continuity conditions for the sound pressure have to be imposed (cf. (PELAT *et al.*, 2009)). The fluid particle velocity $\mathbf{u}_p$ can be expressed at any field point by the acoustic pressure p as follows: $\mathbf{u}_p = (i\omega\rho)^{-1}[\partial p/\partial r, (1/r)\partial p/\partial\varphi, \partial p/\partial z]$. For any fluid particle adjacent to vibrating surface, it has been assumed that $\mathbf{u}_p \mathbf{n} = v_n^{(sur)}$, where $\mathbf{n}$ is the surface normal versor

and $v_n^{(sur)}$ is the normal component of surface velocity. Finally, the following conditions can be formulated

$$\left. \frac{\partial p_1}{\partial r} \right|_{r=a} = 0, \qquad (2)$$

$$\left. \frac{\partial p_1}{\partial z} \right|_{z=0} = i\omega\rho v_b(r,\varphi) = \begin{cases} i\omega\rho v_S(r,\varphi) & \text{for } S, \\ 0 & \text{otherwise,} \end{cases} \qquad (3)$$

$$\left. \frac{\partial p_2}{\partial z} \right|_{z=H} = i\omega\rho v_H(r,\varphi) = \begin{cases} \left. \dfrac{\partial p_1}{\partial z} \right|_{z=H} & \text{for } S_{op}, \\ 0 & \text{otherwise,} \end{cases} \qquad (4)$$

$$p_1(r,\varphi,H) = p_2(r,\varphi,H) \text{ for } S_{op}, \qquad (5)$$

where S is the surface of a sound source, S_{op} is the surface of the cavity opening, $v_b(r,\varphi)$ is the vibration velocity at the cavity bottom, $v_S(r,\varphi)$ describes the vibration velocity of sound source points and $v_H(r,\varphi)$ denotes the vibration velocity in the plane $z = H$. Equations (2) and (3) mean that the cavity walls are perfectly rigid. The continuity for the pressure and the particle velocity at the cavity opening is expressed by Eqs. (4) and (5). Additionally, the condition from Eq. (4) means that the cavity opening is embedded in a perfectly rigid baffle. Taking into account that in the region II, acoustic waves can be propagated to infinity, the following radiation conditions have to be also satisfied (SOMMERFELD, 1964)

$$\begin{aligned} \lim_{R\to\infty} p_2 &= 0, \\ \lim_{R\to\infty} \left[R\left(\frac{\partial p_2}{\partial R} - ikp_2 \right) \right] &= 0, \end{aligned} \qquad (6)$$

where $R = \sqrt{r^2 + (z-H)^2}$. The Helmholtz equation from Eq. (1) and the conditions given by Eqs. (2)–(6) define the sound radiation problem which will be solved.

3. Sound pressure

The sound pressure in the region I, similarly as in the case of the cylindrical duct (cf. (MORSE, INGARD, 1968)), can be presented in the following form

$$\begin{aligned} p_1(r,\varphi,z) = \sum_{m=0}^{\infty} \sum_{n=1}^{\infty} \Big[&\chi_{m,n}^{(c)}(z)\cos(m\varphi) \\ &+ \chi_{m,n}^{(s)}(z)\sin(m\varphi) \Big] J_m(k_{m,n}r), \end{aligned} \qquad (7)$$

where J_m is the Bessel function of order m, $k_{m,n}a = g_{m,n}$, $k_{m,n}$ is the wave number of the cavity mode (m,n), $g_{m,n}$ is the eigenvalue related to the cavity

mode (m,n) calculated from the following eigenequation

$$mJ_m(g_{m,n}) = g_{m,n}J_{m+1}(g_{m,n}), \qquad (8)$$

and $\chi_{m,n}^{(c)}(z)$ and $\chi_{m,n}^{(s)}(z)$ are the functions to be found. The proposed solution from Eq. (7) satisfies the boundary condition given by Eq. (2). Then, inserting Eq. (7) into Eq. (1) results in

$$\frac{\partial^2 \chi_{m,n}^{(u)}(z)}{\partial z^2} + \gamma_{m,n}^2 \chi_{m,n}^{(u)}(z) = 0, \qquad (9)$$

where $u \in \{c,s\}$, $\gamma_{m,n}^2 = k^2 - k_{m,n}^2$. The solution of the above equation can be formulated as

$$\chi_{m,n}^{(u)}(z) = A_{m,n}^{(u)}e^{i\gamma_{m,n}z} + B_{m,n}^{(u)}e^{-i\gamma_{m,n}z}, \qquad (10)$$

where the constants $A_{m,n}^{(u)}$ and $B_{m,n}^{(u)}$ are unknown. The vibration velocity at the cavity bottom can be written in the following form

$$\begin{aligned} v_b(r,\varphi) = \sum_{m=0}^{\infty} \sum_{n=1}^{\infty} \Big[&\vartheta_{m,n}^{(c)}\cos(m\varphi) \\ &+ \vartheta_{m,n}^{(s)}\sin(m\varphi) \Big] J_m(k_{m,n}r), \end{aligned} \qquad (11)$$

where

$$\vartheta_{m,n}^{(c)} = \frac{\varepsilon_m}{2\pi N_{m,n}} \int_S v_S(r,\varphi)\cos(m\varphi)J_m(k_{m,n}r)\,\mathrm{d}S,$$

$$\vartheta_{m,n}^{(s)} = \frac{1}{\pi N_{m,n}} \int_S v_S(r,\varphi)\sin(m\varphi)J_m(k_{m,n}r)\,\mathrm{d}S, \qquad (12)$$

S is the sound source surface, $\varepsilon_m = 1$ for $m = 0$ and $\varepsilon_m = 2$ when $m > 0$, and

$$N_{m,n} = \frac{a^2}{2}\left(1 - \frac{m^2}{g_{m,n}^2}\right)J_m^2(g_{m,n}). \qquad (13)$$

Using Eqs. (7) and (11) and employing the boundary condition from Eq. (3) leads to

$$B_{m,n}^{(u)} = A_{m,n}^{(u)} - \frac{\omega\rho\vartheta_{m,n}^{(u)}}{\gamma_{m,n}},$$

and

$$\chi_{m,n}^{(u)}(z) = 2A_{m,n}^{(u)}\cos(\gamma_{m,n}z) - \frac{\omega\rho\vartheta_{m,n}^{(u)}e^{-i\gamma_{m,n}z}}{\gamma_{m,n}}. \qquad (14)$$

Taking into account that the value of the sound pressure has to be finite, it is necessary to assume that $\gamma_{m,n} = \sqrt{k^2 - k_{m,n}^2}$ for $k > k_{m,n}$ and $\gamma_{m,n} = -i\sqrt{k_{m,n}^2 - k^2}$ when $k < k_{m,n}$.

Making use of the Fourier series and the Hankel transform (DEBNATH, BHATTA, 2015), the sound pressure in the region II can be written as follows

$$p_2(r, \varphi, z) = \sum_{m=0}^{\infty} \Big[G_m^{(c)}(r, z) \cos(m\varphi)$$
$$+ G_m^{(s)}(r, z) \sin(m\varphi) \Big], \quad (15)$$

where

$$G_m^{(u)}(r, z) = \int_0^{\infty} K_m^{(u)}(\tau, z) J_m(\tau r) \tau \, \mathrm{d}\tau, \quad (16)$$

and the functions $K_m^{(u)}(\tau)$ are to be determined. Inserting the above solution into the Helmholtz equation given by Eq. (1) yields

$$\frac{\partial^2 K_m^{(u)}(\tau, z)}{\partial z^2} + \mu^2 K_m^{(u)}(\tau, z) = 0, \quad (17)$$

where $\mu^2 = k^2 - \tau^2$ with the following convention introduced $\mu = \sqrt{k^2 - \tau^2}$ for $k > \tau$ and $\mu = i\sqrt{\tau^2 - k^2}$ for $k < \tau$. The solution of Eq. (17), for which the value of p_2 is finite when $z \to \infty$, can be expressed as

$$K_m^{(u)}(\tau, z) = C_m^{(u)}(\tau) e^{i\mu z}, \quad (18)$$

where the functions $C_m^{(u)}(\tau)$ are unknown. Using the Fourier series and the Hankel transform, and based on Eqs. (4), (7) and Eq. (14), the vibration velocity in the plane $z = H$ can be written in the following form

$$v_H(r, \varphi) = \sum_{m=0}^{\infty} \Big[T_m^{(c)}(r) \cos(m\varphi)$$
$$+ T_m^{(s)}(r) \sin(m\varphi) \Big], \quad (19)$$

where

$$T_m^{(u)}(r) = \sum_{n=1}^{\infty} U_{m,n}^{(u)} \int_0^{\infty} V_{m,n}(\tau) J_m(\tau r) \tau \, \mathrm{d}\tau, \quad (20)$$

and

$$V_{m,n}(\tau) = \int_0^a J_m(k_{m,n} r) J_m(\tau r) r \, \mathrm{d}r$$
$$= \frac{a^2}{g_{m,n}^2 - (\tau a)^2} \big[g_{m,n} J_m(\tau a) J_{m+1}(g_{m,n})$$
$$- \tau a J_m(g_{m,n}) J_{m+1}(\tau a) \big], \quad (21)$$

and

$$U_{m,n}^{(u)} = \frac{-2\gamma_{m,n} A_{m,n}^{(u)} \sin(\gamma_{m,n} H)}{i\omega\rho} + \vartheta_{m,n}^{(u)} e^{-i\gamma_{m,n} H}. \quad (22)$$

Combining Eqs. (15), (18), (19) and (20) and taking into account the conditions from Eq. (4) yields

$$C_m^{(u)}(\tau) = \omega\rho \sum_{n=1}^{\infty} \frac{U_{m,n}^{(u)} V_{m,n}(\tau) e^{-i\mu H}}{\mu}. \quad (23)$$

Finally, using Eqs. (15), (18) and (23), the sound pressure outside the cavity can be written in the following form

$$p_2(r, \varphi, z) = \omega\rho \sum_{m=0}^{\infty} \sum_{n=1}^{\infty} \Big[U_{m,n}^{(c)} \cos(m\varphi)$$
$$+ U_{m,n}^{(s)} \sin(m\varphi) \Big] L_{m,n}(r, z), \quad (24)$$

where

$$L_{m,n}(r, z) = \int_0^{\infty} \frac{V_{m,n}(\tau)}{\mu} e^{i\mu(z-H)} J_m(\tau r) \tau \, \mathrm{d}\tau. \quad (25)$$

On the basis of Eqs. (7) and (24), it should be noted that the continuity condition given by Eq. (5) is satisfied when

$$\sum_{q=1}^{\infty} \chi_{m,q}^{(u)}(H) J_m(k_{m,q} r) = \omega\rho \sum_{q=1}^{\infty} U_{m,q}^{(u)} L_{m,q}(r, H) \quad (26)$$

for $0 \le r \le a$.

Then, multiplying the above equation by $J_m(k_{m,n} r) r$, integrating over r from 0 to a, and making use of the following orthogonality property

$$\int_0^a J_m(k_{m,n} r) J_m(k_{m,q} r) r \, \mathrm{d}r = N_{m,n} \delta_{n,q},$$

where $\delta_{n,q}$ is the Kronecker delta, results in

$$\chi_{m,n}^{(u)}(H) = \frac{\omega\rho}{N_{m,n}} \sum_{q=1}^{\infty} U_{m,q}^{(u)} \xi_{m,n,q}, \quad (27)$$

where

$$\xi_{m,n,q} = \int_0^{\infty} \frac{V_{m,n}(\tau) V_{m,q}(\tau) \tau \, \mathrm{d}\tau}{\mu}. \quad (28)$$

Inserting Eqs. (14) and (22) into Eq. (27) leads to the following set of equations

$$2A_{m,n}^{(u)} \cos(\gamma_{m,n} H) - \frac{2i}{N_{m,n}}$$
$$\cdot \sum_{q=1}^{\infty} \gamma_{m,q} A_{m,q}^{(u)} \sin(\gamma_{m,q} H) \xi_{m,n,q} = \omega\rho Q_{m,n}, \quad (29)$$

where $m = 0, 1, 2, ..., n = 1, 2, 3, ...,$ and

$$Q_{m,n} = \frac{\vartheta_{m,n}^{(u)}}{\gamma_{m,n}} e^{-i\gamma_{m,n} H}$$
$$+ \frac{1}{N_{m,n}} \sum_{q=1}^{\infty} \Big(\vartheta_{m,q}^{(u)} e^{-i\gamma_{m,q} H} \xi_{m,n,q} \Big). \quad (30)$$

Based on the set of equations from Eq. (29), the constants $A_{m,n}^{(u)}$ can be calculated. Then, the sound pressure inside the cavity can be determined with the use of the formulas given by Eqs. (7) and (14), and the sound pressure outside the cavity can be obtained by using Eq. (24).

4. Approximated formula for the sound pressure in the far field

To determine the sound pressure outside the cavity based on Eq. (24), it is necessary to calculate the integrals given by Eq. (25) which is time consuming especially when a large number of cavity modes is used. Hence, it is of great practical importance to obtain an approximated formula for the quantity p_2. It is possible for the field points located at a great distance from the cavity opening. Introducing the spherical coordinate system $(r_s, \theta_s, \varphi_s)$ with the origin at the central point of the cavity opening, i.e. at the point $(0, 0, H)$ of the Cartesian coordinate system, the sound pressure in the region II can be formulated as follows (see (SZEMELA, 2017))

$$p_2(r_s, \theta_s, \varphi_s) = -\frac{i\omega\rho}{2\pi} \int\limits_0^a \int\limits_0^{2\pi} v_{op}(r_0, \varphi_0)$$
$$\cdot \frac{e^{ikR}}{R} \, d\varphi_0 r_0 \, dr_0, \qquad (31)$$

where $v_{op}(r_0, \varphi_0)$ is the distribution of vibration velocity at the cavity opening in polar coordinates, and

$$R = \sqrt{r_s^2 + r_0^2 - 2r_s r_0 \sin\theta_s \cos(\varphi_s - \varphi_0)}, \qquad (32)$$

is the distance between the fixed point of the cavity opening and the fixed field point. Taking into account that $v_{op} = -\frac{i}{\omega\rho}\frac{\partial p_1}{\partial z}\Big|_{z=H}$ and using Eqs. (7) and (14) results in

$$v_{op}(r_0, \varphi_0) = \sum_{m=0}^{\infty} \sum_{n=1}^{\infty} \Big[U_{m,n}^{(c)} \cos(m\varphi_0)$$
$$+ U_{m,n}^{(s)} \sin(m\varphi_0) \Big] J_m(k_{m,n}r_0). \quad (33)$$

In the case of the far field, i.e., when $r_s \gg a$, the following approximation can be used (cf. (MORSE, INGARD, 1968))

$$\frac{e^{ikR}}{R} \approx \frac{e^{ik(r_s - r_0 \sin\theta_s \cos(\varphi_s - \varphi_0))}}{r_s}. \qquad (34)$$

Then, inserting Eqs. (33) and (34) into Eq. (31) and performing integration with the use of the following series (MCLACHLAN, 1955)

$$\cos(w\cos\alpha) = \sum_{s=0}^{\infty} \varepsilon_s(-1)^s J_{2s}(w)\cos(2s\alpha),$$
$$\sin(w\cos\alpha) = 2\sum_{s=0}^{\infty}(-1)^s J_{2s+1}(w)\cos\left[(2s+1)\alpha\right], \qquad (35)$$

yields

$$p_2^{(a)}(r_s, \theta_s, \varphi_s) = \frac{(-i)^{m+1}\omega\rho\, e^{ikr_s}}{r_s}$$
$$\cdot \sum_{m=0}^{\infty} \sum_{n=1}^{\infty} \Big[U_{m,n}^{(c)} \cos(m\varphi_s)$$
$$+ U_{m,n}^{(s)} \sin(m\varphi_s) \Big] V_{m,n}(k\sin\theta_s), (36)$$

where $p_2^{(a)}$ is the approximated value of the sound pressure in the far field. Using Eq. (36) the calculations time for the quantity p_2 can be significantly reduced in the case of field points located at a great distance from the cavity opening.

5. Sound power

The time-averaged sound power radiated by the considered vibroacoustic system can be expressed as (cf. (RDZANEK *et al.*, 2016))

$$\Pi = \frac{1}{2} \int\limits_S p_1(r, \varphi, 0) v_S^*(r, \varphi) \, dS, \qquad (37)$$

where the symbol $*$ denotes the conjugate of a complex quantity. Making use of Eq. (7) and (14), the above formula can be written in the following form

$$\Pi = \Pi_a + i\Pi_r = \pi \sum_{m=0}^{\infty} \sum_{n=1}^{\infty} N_{m,n} \left[\frac{F_{m,n}^{(c)}}{\varepsilon_m} + \frac{F_{m,n}^{(s)}}{2} \right], \quad (38)$$

where Π_a and Π_r denote the active and reactive sound power, respectively, and

$$F_{m,n}^{(u)} = \left(2A_{m,n}^{(u)} - \frac{\omega\rho\, \vartheta_{m,n}^{(u)}}{\gamma_{m,n}} \right) \vartheta_{m,n}^{(u)*}. \qquad (39)$$

The formula in Eq. (38) can be used for the sound power calculations. However, for this purpose, the coefficients $\xi_{m,n,q}$ from Eq. (28) have to be calculated. This allows the values of the constants $A_{m,n}^{(u)}$ to be determined by using the set of equations given by Eq. (29).

6. Sound radiation by a rectangular piston

As an example, the presented formulas have been used to predict an acoustic behavior of the considered vibroacoustic system with a vibrating rectangular piston located at the cavity bottom. The location of sound

source central point is determined by the two coordinates d_x and d_y of the Cartesian coordinate system (see Fig. 1). The lengths of piston sides are equal to l_x and l_y, and the side with the length l_x is parallel to the x axis. The sound source vibrations are time harmonic with the amplitude v_0. In order to use the presented formulas for the sound pressure and sound power, it is necessary to truncate the infinite sums which means that only some cavity modes (m, n) can be taken into account in the numerical calculations. This leads to the truncation error. It has been assumed that all the cavity modes of the modal numbers $m, n \leq W$, where W is the truncation constant, have been employed in the numerical simulations. The truncation error can be estimated as follows

$$E = \frac{|V_{2q} - V_q|}{|V_{2q}|} \cdot 100\%, \qquad (40)$$

where V_q is the value of quantity calculated when all the cavity modes (m, n) with modal numbers $m, n \leq q$ have been used in the calculations. The appropriate value of W can be found by analyzing the value of the truncation error.
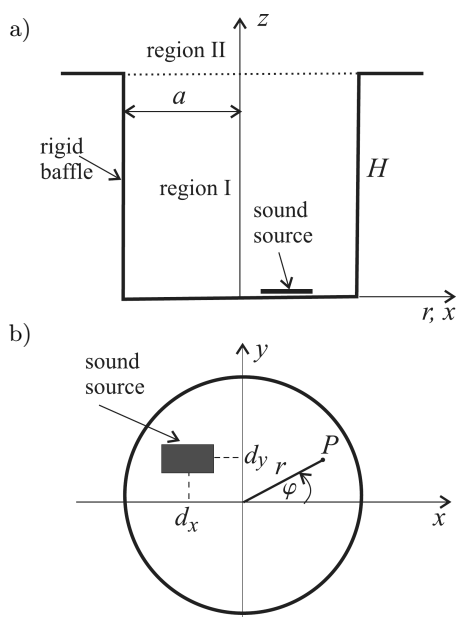
a)

b)

Fig. 1. The considered vibroacoustic system: a) connected regions: open cavity and the half space, b) cavity cross-section with the rectangular piston located at the bottom and the cylindrical coordinates r and φ of the field point P.

To analyze the sound radiation in the case of the considered open cavity, it is necessary to calculate the coefficients $\xi_{m,n,q}$ from Eq. (28) and then to solve the set of equations given by Eq. (29). The calculations of $\xi_{m,n,q}$ can be improved by using the following relation $\xi_{m,n,q} = \xi_{m,q,n}$. The normalized sound pressure p/p_0 and the normalized sound power Π/Π_0, where p denotes p_1 or p_2, $p_0 = c\rho v_0$ and $\Pi_0 = c\rho S v_0^2/2$, can be expressed by the following dimensionless parameters:

l_x/a, l_y/a, d_x/a, d_y/a, cavity depth ratio H/a and the normalized angular frequency ka. In this study, the numerical analysis has been performed for the normalized sound pressure modulus and the radiation efficiency $\sigma = \Pi_a/\Pi_0$. The three selected piston locations have been analyzed: the location I – $d_x/a = d_y/a = 0$, the location II – $d_x/a = 0.5$ and $d_y/a = 0$, and the location III – $d_x/a = d_y/a = 0.5$.

6.1. Sound pressure

On the basis of Eqs. (7), (14) and (24), the normalized sound pressure modulus has been analyzed in the case when $l_x/a = 0.1$, $l_y/a = 0.05$ and $H/a = 2$. Taking into account that the lowest eigenvalues of the considered cavity equal $g_{0,1} = 0$, $g_{1,1} = 1.84$, $g_{2,1} = 3.05$, $g_{0,2} = 3.83$ and $g_{3,1} = 4.20$, the numerical calculations have been performed for $ka = 1.3$, 2.6 and 9.1 so that the sound radiation can be investigated in the cases when: only mode $(0, 1)$ is cut on mode, only modes $(0, 1)$ and $(1, 1)$ are propagated and a greater number of cut on modes occur. In Figs. 2–6, the distributions of the normalized sound pressure modulus have been presented for the surfaces $z = H/2$ and $z = 3H/2$. To determine the appropriate value of truncation con-
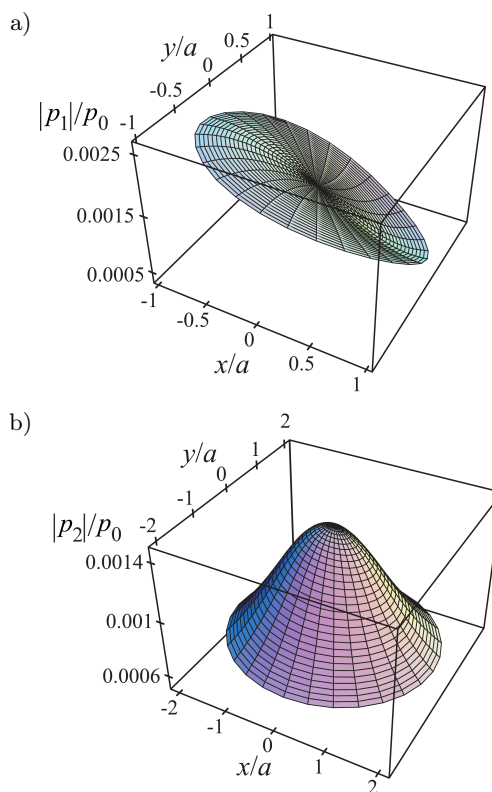
a)

b)

Fig. 2. The distribution of normalized sound pressure modulus: a) $|p_1|/p_0$ inside the cavity for $z = H/2$ ($E_{avg} = 0.23\%$), b) $|p_2|/p_0$ outside the cavity for $z = 3H/2$ ($E_{avg} = 0.04\%$). It has been assumed that $ka = 1.3$, $W = 3$ and the piston location III.
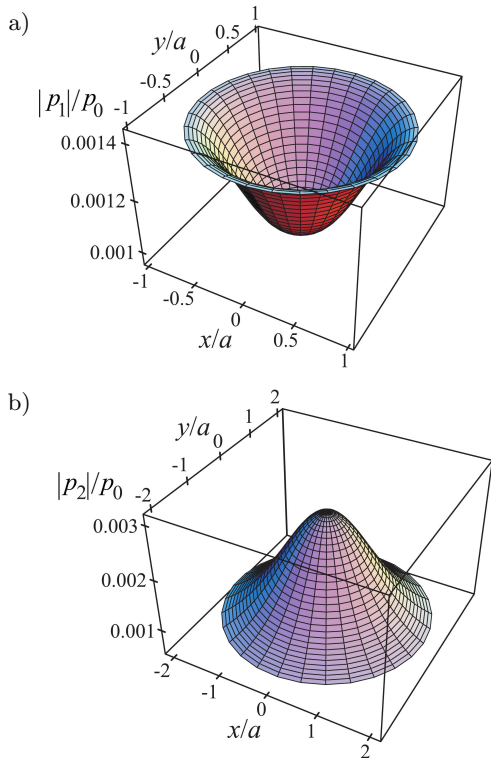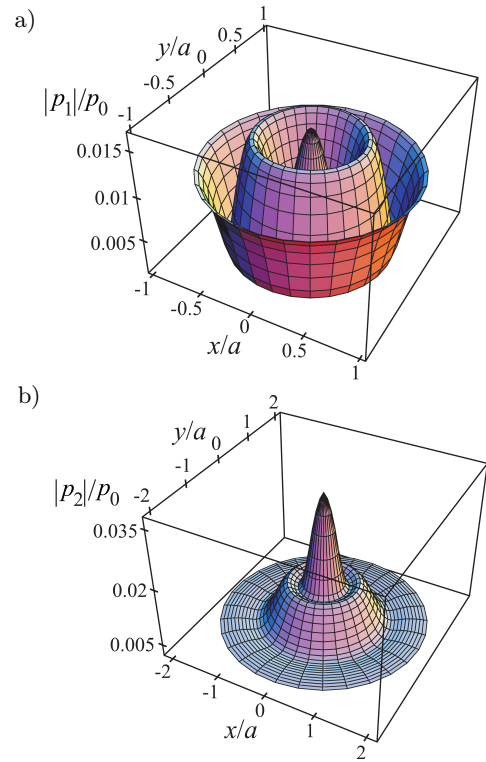
a)

b)

Fig. 3. The distribution of normalized sound pressure modulus: a) $|p_1|/p_0$ inside the cavity for $z = H/2$ ($E_{avg} = 0.09\%$), b) $|p_2|/p_0$ outside the cavity for $z = 3H/2$ ($E_{avg} = 0.11\%$). It has been assumed that $ka = 2.6$, $W = 5$ and the piston location I.
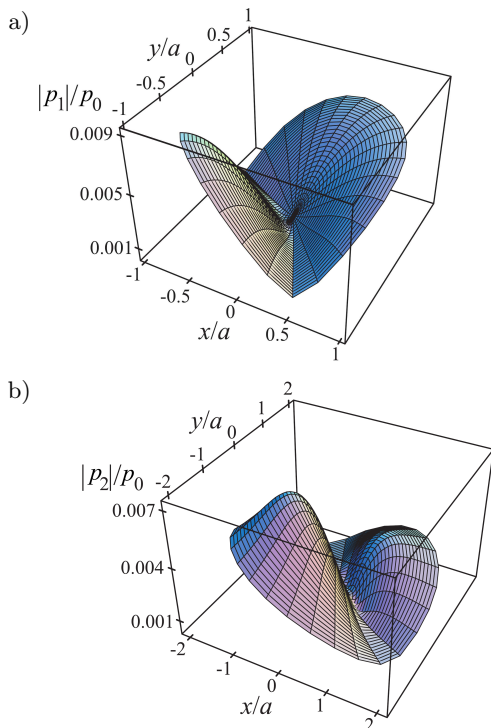
a)

b)

Fig. 5. The distribution of normalized sound pressure modulus: a) $|p_1|/p_0$ inside the cavity for $z = H/2$ ($E_{avg} = 0.41\%$), b) $|p_2|/p_0$ outside the cavity for $z = 3H/2$ ($E_{avg} = 0.36\%$). It has been assumed that $ka = 9.1$, $W = 8$ and the piston location I.

a)

b)

Fig. 4. The distribution of normalized sound pressure modulus: a) $|p_1|/p_0$ inside the cavity for $z = H/2$ ($E_{avg} = 0.24\%$), b) $|p_2|/p_0$ outside the cavity for $z = 3H/2$ ($E_{avg} = 0.44\%$). It has been assumed that $ka = 2.6$, $W = 5$ and the piston location III.
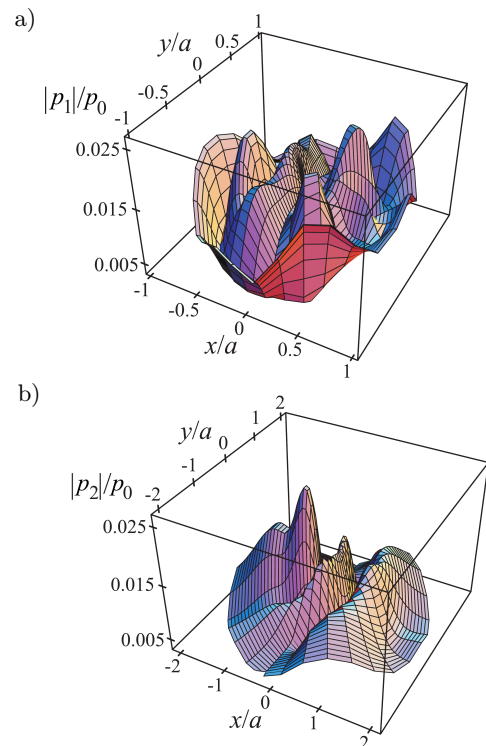
a)

b)

Fig. 6. The distribution of normalized sound pressure modulus: a) $|p_1|/p_0$ inside the cavity for $z = H/2$ ($E_{avg} = 0.20\%$), b) $|p_2|/p_0$ outside the cavity for $z = 3H/2$ ($E_{avg} = 0.28\%$). It has been assumed that $ka = 9.1$, $W = 8$ and the piston location II.

stant W, the following average truncation error has been analyzed

$$E_{avg} = \sum_{j=1}^{N} E_j/N, \qquad (41)$$

where E_j denote the value of truncation error from Eq. (40) calculated for a fixed field point and N is the number of considered field points.

For all the presented in Figs. 2–6 distributions of sound pressure modulus, the average truncation error $E_{avg} < 0.5\%$ which proves that the obtained results are accurate enough to be discussed. The values of E_{avg} and truncation constant W have been given in the figure descriptions. Figures 3 and 5 show that the distribution of acoustic field inside as well as outside the cavity is almost axisymmetric for the piston location I. This means that a sound source with an arbitrary shape located at the central point of cavity bottom can emit a nearly axisymmetric acoustic radiation. For the piston location II and III, the distributions of the quantities $|p_1|$ and $|p_2|$ are more complicated. Figure 2 shows that when $ka = 1.3$, the distribution of the sound pressure modulus inside the cavity is asymmetric with one maximum and one minimum, while the distribution of this quantity outside the cavity is nearly axisymmetric. This demonstrates that the sound radiation inside the cavity is strongly influenced by the asymmetric cut off modes. However, above the cavity opening, the fundamental mode $(0, 1)$ gives the greatest contribution to the acoustic field. For the higher frequencies, a greater number maxima and minima of the sound pressure modulus are observed at some field points (see Figs. 4 and 6). This effect is due to the interference of short acoustic waves radiated directly by the sound source and those reflected from the cavity wall.

Based on the approximated formula from Eq. (36), the distribution of sound pressure modulus in the far field can be determined. To compare the exact value of $|p_2|$ with its approximated value $|p_2^{(a)}|$, the following relative error

$$E_a = \frac{\left| |p_2| - |p_2^{(a)}| \right|}{|p_2|} \cdot 100\%, \qquad (42)$$

can be used. In Fig. 7, the quantity $|p_2^{(a)}|$ and the corresponding relative error E_a have been presented as the functions of the spherical coordinate θ_s. The approximated values of the sound pressure modulus have not been illustrated at the field points with $\theta_s = \pi/2$ which is due to some great values of E_a. The numerical analysis has been performed for some selected values of the spherical coordinate r_s. The truncation error E given by Eq. (40) estimated at all the analyzed field points is less than 0.3% for $ka = 1.3$ and does not exceed 1.1% when $ka = 2.6$. This proves that the value of W
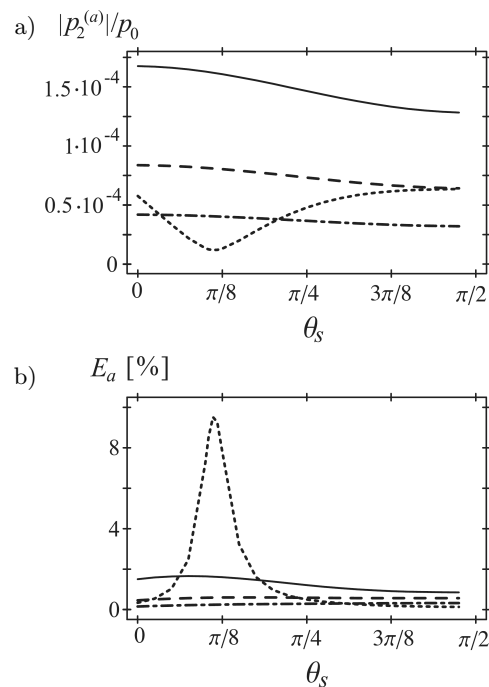

a) $|p_2^{(a)}|/p_0$

b) $E_a\ [\%]$

Fig. 7. The normalized sound pressure modulus in the far field $|p_2^{(a)}|/p_0$ as a function of the spherical coordinate θ_s for $\varphi_s = 0$ and the piston location III. The line keys: solid – $ka = 1.3$, $W = 3$ and $r_s = 5a$ ($t_r^{(avg)} = 230$), dashed – $ka = 1.3$, $W = 3$ and $r_s = 10a$ ($t_r^{(avg)} = 390$), dashed-dotted – $ka = 1.3$, $W = 3$ and $r_s = 20a$ ($t_r^{(avg)} = 430$), and dotted – $ka = 2.6$, $W = 8$ and $r_s/a = 30$ ($t_r^{(avg)} = 440$).

has been correctly chosen. In the case of $ka = 1.3$, the sound pressure modulus in the far field slightly varies with the value of θ_s (see Fig. 7a). The quantity $|p_2^{(a)}|$ is significantly influenced by the value of θ_s when $ka = 2.6$ and $r_s = 30a$. In this case, the minimal value of the sound pressure modulus occurs when θ_s is equal to about $\pi/8$. Some greater values of $|p_2^{(a)}|$ are observed when θ_s is close to zero which can be due to acoustic waves propagated directly by a sound source located at the cavity bottom. Moreover, the value of sound pressure modulus increases as θ_s tends to $\pi/2$ which can be caused by the additional contribution of acoustic waves reflected from the flat baffle in which the cavity is embedded. Figure 7b proves that the approximated formula from Eq. (36) is accurate enough to be useful for the calculations of sound pressure modulus in the far field. The increase in the value of r_s causes that the approximated value $|p_2^{(a)}|$ becomes more accurate. This effect has been illustrated in Fig. 7b for $ka = 1.3$. The value of E_a is less than 1.7% for $r_s = 5a$, $E_a < 0.6\%$ if $r_s = 10a$ and E_a does not exceed about 0.3% when $r_s = 20a$. Moreover, the formula from Eq. (36) can also be employed for higher frequencies. For example, it is possible to obtain the approximated value of $|p_2|$ for $ka = 2.6$. The relative error E_a is less than 4% when $r_s = 30a$. The exception is the narrow range of θ_s in

which the value of sound pressure modulus is close to zero.

The approximated formulas are used to reduce calculations time. Hence, it is of practical importance to compare the computational efficiency of the approximated formula with the computational efficiency of the exact one. For this purpose, the following average relative calculations time has been defined

$$t_r^{(avg)} = \frac{1}{N} \sum_{j=1}^{N} \frac{t_e^{(j)}}{t_a^{(j)}}, \quad (43)$$

where N is the number of analyzed field points and $t_e^{(j)}$ and $t_a^{(j)}$ are calculations times of the sound pressure modulus at the fixed field point with the use of the approximated and exact formula, respectively. Estimating the times $t_e^{(j)}$ and $t_a^{(j)}$, it has been assumed that the necessary values of constants $A_{m,n}^{(u)}$ are calculated and can be used for the calculations of quantity $|p_2|$ and $|p_2^{(a)}|$. The average relative calculations time $t_r^{(avg)}$ has been determined for all the curves presented in Fig. 7a and its values have been given in the description of this figure. It has been estimated that the approximated formula given by Eq. (36) allows the calculations time to be reduced even more than 400 times for $ka = 1.3$ as well as $ka = 2.6$. This shows a high computational efficiency of the obtained approximated formula.

6.2. Radiation efficiency

The formula from Eq. (38) can be used to calculate the radiation efficiency σ as well as the normalized reactive sound power Π_r/Π_0. Taking into account that the radiation efficiency can be measured, this quantity is interesting from a practical point of view. The series given by Eq. (38) is fast convergent for the real part and slowly convergent for the imaginary one. This causes that the numerical calculations of Π_r are troublesome and time consuming. Therefore, only the radiation efficiency has been analyzed in this study.

The formula given by Eq. (38) is valid for the cavity of any depth H including also the specific case of $H = 0$, i.e., when a sound source is embedded in a flat rigid baffle. The radiation efficiency of a baffled rectangular piston σ_b can be obtained based on (ZAWIESKA, RDZANEK, 2007) and expressed as follows

$$\sigma_b = \frac{1}{4\pi^2 k^2 l_x l_y} \int\limits_0^1 \int\limits_0^{2\pi} \frac{M(\tau, \alpha) M^*(\tau, \alpha)}{\sqrt{1 - \tau^2}} \tau \, d\tau \, d\alpha, \quad (44)$$

where

$$M(\tau, \alpha) = \frac{2 \left(1 - e^{-ikl_x \tau \cos \alpha}\right) \left(1 - e^{-ikl_y \tau \sin \alpha}\right)}{\tau^2 \sin 2\alpha}. \quad (45)$$

The formula for σ is more complicated and has a lower computational efficiency than the formula obtained for a baffled sound source. Moreover, it is obvious that the radiation efficiency of the cavity with a sound source located at its bottom assumes similar value as the radiation efficiency of the same source embedded in a rigid baffle when the cavity depth H is small enough. Hence, it is of practical importance to determine the value of depth ratio H/a for which the radiation efficiency of the analyzed vibroacoustic system can be approximately calculated from the less complicated formula valid for baffled piston. In particular, the formula from (44) can also be used to check the validity of the presented solution for $H = 0$. To conveniently perform a further analysis, the following relative error E_b has been defined

$$E_b = \frac{|\sigma_b - \sigma|}{\sigma_b} \cdot 100\%. \quad (46)$$

The above quantity has been analyzed as a function of the normalized angular frequency ka within the limits $ka \in (0, 13)$ for pistons with different lengths of sides assuming that $l_y = l_x/2$. Moreover, some selected sound source locations have been considered. To check the validity of the formula form Eq. (38), the relative error E_b has been analyzed when $H = 0$. The investigations have been performed for the truncation constant $W = 30$ and $l_x/a = 0.05, 0.1, 0.2$, and 0.4. The calculated values of E_b are less than 0.05% for all the analyzed cases. This shows that the results obtained for the piston located at the bottom of cavity with $H = 0$ agree with those obtained for the baffled piston. Some small differences between the calculated values can be caused by the use of finite number of cavity modes as well as by some numerical errors. In Figs. 8 and 9, the quantity E_b has been presented as a function of ka for $H/a = 0.01$ and 0.05. The behavior of E_b for two selected pistons has been illustrated in Fig. 8 while Fig. 9 shows the values of E_b in the case of two different pis-
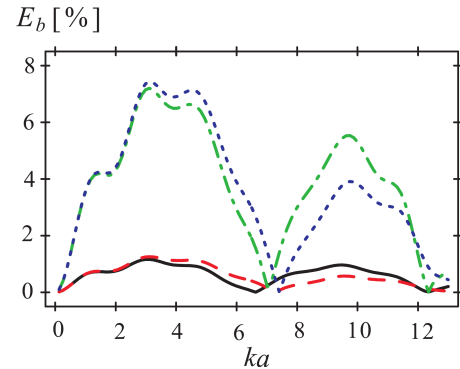

Fig. 8. The relative error E_b given by Eq. (46) as a function of the normalized angular frequency ka for the piston location III, $l_y = l_x/2$ and $W = 15$. The line keys: solid – $H = 0.01a$ and $l_x = 0.1a$, dashed – $H = 0.01a$ and $l_x = 0.4a$, dashed-dotted – $H = 0.05a$ and $l_x = 0.1a$, and dotted – $H = 0.05a$ and $l_x = 0.4a$.
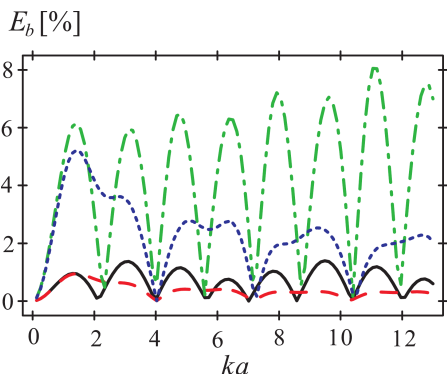
Fig. 9. The relative error E_b given by Eq. (46) as a function of the normalized angular frequency ka for $l_x/a = 0.1$, $l_y/a = 0.05$ and $W = 15$. The line keys: solid – the piston location I and $H/a = 0.01$, dashed – the piston location II and $H/a = 0.01$, dashed-dotted – the piston location I and $H/a = 0.05$ and dotted – the piston location II and $H/a = 0.05$.

ton locations. It can be concluded that the radiation efficiency of cavity when its depth ratio $H/a \leq 0.01$, can be calculated from the less complicated formula given by Eq. (44) with the relative error E_b less than about 1.4%. The value of σ can also be estimated based on the formula valid for baffled piston with the relative error E_b less than about 8% when $H/a = 0.05$ (see Figs. 8 and 9). However, placing the sound source at the bottom of cylindrical resonator instead of in a flat baffle significantly modifies its radiation efficiency in the case of $H/a > 0.05$.

The damping effects have been neglected in this study. However, they play an essential role in the case of the resonance frequencies and therefore, the quantity σ has not been calculated for $ka = g_{m,n}$. In Fig. 10, the radiation efficiency of baffled piston and the radiation efficiency σ for the depth ratio $H/a = 0.2$, 0.5, and 2 have been presented as the functions of ka. The quan-
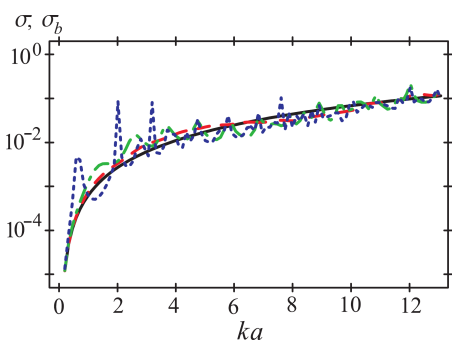

Fig. 10. The radiation efficiency of the rectangular piston σ_b and the radiation efficiency of the cylindrical cavity σ as the functions of the normalized angular frequency ka for the piston location III, $l_x/a = 0.1$, $l_y/a = 0.05$ and $W = 15$. The line keys: solid – σ_b, dashed – σ for $H/a = 0.2$, dashed-dotted – σ for $H/a = 0.5$ and dotted – σ for $H/a = 2$.

tity σ has been calculated with the acceptable value of the truncation error E which does not exceed 0.46%. Figure 10 exhibits that the acoustic behavior of considered cavity strongly depends on its depth. In the case when $H/a \geq 0.5$, the resonator in the form of open cavity causes that the maxima of radiation efficiency occur for some values of ka. This effect, similarly as in the case of the baffled piston, is not observed for the shallow cavity with $H/a \leq 0.2$ (see Fig. 10). At low frequencies, when $ka < 0.25$, the quantities σ and σ_b assume some similar values even in the case of the deep cavity with depth ratio $H/a = 2$.

The quantity σ as a function of ka has been presented in Fig. 11 for some selected piston locations with the truncation error $E < 0.44\%$. It is noteworthy that the influence of piston location on the value of σ is significant only when $ka > 1.6$ (see Fig. 11). This acoustic behavior can be explained by the fact that in the case when $ka < g_{1,1}$ only the cavity mode $(0, 1)$ is the cut on mode. Hence, only acoustic waves related to this mode are propagated. Thus, it can been concluded that the acoustic energy propagated by the fundamental mode at low frequencies does not considerably depend on the piston location and the acoustic power emitted by the higher evanescent modes is negligible small. When $ka > g_{1,1}$, the influence of piston location on the radiation efficiency can be significant. For example, when $2 < ka < 3.5$, the quantity σ assumes greater values for the piston locations II and III than for the piston location I.
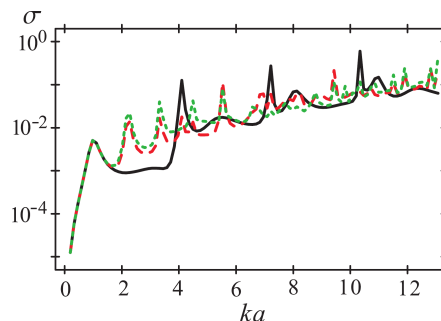

Fig. 11. The radiation efficiency σ as a function of the normalized angular frequency ka for $H/a = 1$, $l_x/a = 0.1$, $l_y/a = 0.05$ and $W = 15$. The line keys: solid – the piston location I, dashed – the piston location II and dotted – the piston location III.

7. Conclusions

Making use of the modal decomposition and the continuity conditions, the rigorous solution describing the sound radiation of the cylindrical open cavity embedded in the rigid infinite baffle has been obtained for the general case of an arbitrary surface sound source located at the cavity bottom. The use of the proposed formulas is an alternative methodology to the finite ele-

ment method. The accuracy of results obtained based on the presented solution depends on the truncation error which is due to the fact that, in practice, only finite number of cavity modes can be used in the numerical calculations.

Additionally, to improve the numerical calculations of the sound pressure outside the cavity, the approximated formula of a high computational efficiency and valid for the far field has been formulated. In order to investigate some general acoustic properties of the considered vibroacoustic system, the numerical analysis has been performed in the case when the sound source is a rectangular piston. The distribution of the sound pressure modulus has been illustrated for some selected piston locations as well as for different values of the normalized angular frequency. The performed numerical simulations have shown that the use of the obtained approximated formula allows the calculations time of the sound pressure modulus to be reduced even more than 400 times.

In order to check the validity of the obtained solution, the radiation efficiency of the piston located at the bottom of cavity with depth equal to zero has been compared with the radiation efficiency of the baffled rectangular piston. An excellent agreement has been achieved. Based on the numerical analysis, it can be concluded that placing the sound source at the bottom of the shallow cavity with depth ratio less than or equal to 0.01 instead of in a flat baffle does not considerably change its radiation efficiency. Hence, the radiation efficiency of shallow cavities can be calculated from the less complicated formula valid for baffled sound source which allows the calculations time to be significantly reduced. The performed numerical investigations demonstrate that the radiation efficiency of the considered cavity is strongly influenced by its depth. For the cavity with depth ratio less than or equal to 0.2, the maxima of radiation efficiency, similarly as in the case of the baffled piston, are not observed for any frequency. They occur in the case of the cavity with depth ratio greater than or equal to 0.5. When the normalized angular frequency is less than 0.25, the radiation efficiencies of cavities with different depths assume similar values as the radiation efficiency of the baffled sound source. The piston location does not considerably influences the radiation efficiency when the normalized angular frequency is smaller than about 1.6. This acoustic behavior is due to the fact that, at low frequencies, the greatest contribution to the radiation efficiency has the fundamental cavity mode and the acoustic energy radiated by this mode is not significantly dependent on the piston location.

Although the numerical analysis has been performed assuming that the sound source is the rectangular piston, the formulated herein conclusions show the nature and some general properties of the considered vibroacoustic system.

References

1. BHUDDI A., GOBERT M.-L., MENCIK J.-M. (2015), *On the acoustic radiation of axisymmetric fluid-filled pipes using the wave finite element (WFE) method*, Journal of Computational Acoustics, **23**, 1550011 (34 pages).

2. CHOI W., WOODHOUSE J., LANGLEY R.S. (2014), *Sound radiation from a vibrating plate with uncertainty*, Journal of Sound and Vibration, **333**, 3966–3980.

3. DEBNATH L., BHATTA D. (2015), *Integral transforms and their applications*, CRC Press Taylor & Francis Group, New York.

4. GONZÁLEZ L.M., COBO P., THEOFILIS V., VALERO E. (2013), *Acoustic resonances in 2D open cavities*, Acta Acustica united with Acustica, **99**, 4, 572–581.

5. HASHEMINEJAD S.M., SHAKERI R., REZAEI S. (2012), *Vibro-acoustic response of an elliptical plate-cavity coupled system to external shock loads*, Applied Acoustics, **73**, 757–769.

6. JEONG U.-C, KIM J.-S., KIM Y.-D., OH J.-E. (2016), *Reduction of radiated exterior noise from the flexible vibrating plate of a rectangular enclosure using multi-channel active control*, Applied Acoustics, **105**, 45–54.

7. JURKIEWICZ J., SNAKOWSKA A., SMOLIK D. (2011), *Acoustic impedance of outlet of a hard-walled unbaffled cylindrical duct for multimode incident wave*, Acta Physica Polonica A, **119**, 6A, 1061–1067.

8. KARBAN U., SCHRAM C., SOVARDI C., POLIFKE W. (2016), *Tailored Green's functions for the prediction of the noise generated by single and tandem diaphragms in a circular duct*, Acta Acustica united with Acustica, **102**, 5, 779–792.

9. LEE P.J., KANG J. (2015), *Effect of height-to-width ratio on the sound propagation in urban streets*, Acta Acustica united with Acustica, **101**, 1, 73–87.

10. LENIOWSKA L., MAZAN D. (2015), *MFC sensors and actuators in active vibration control of the circular plate*, Archives of Acoustics, **40**, 2, 257–265.

11. MAZUR K., PAWEŁCZYK M. (2016), *Internal model control for a light-weight active noise-reducing casing*, Archives of Acoustics, **41**, 2, 315–322.

12. MCLACHLAN N.W. (1955), *Bessel functions for engineers*, Clarendon Press, Oxford.

13. MEISSNER M. (2013), *Acoustic behaviour of lightly damped rooms*, Acta Acustica united with Acustica, **99**, 5, 845–847.

14. MORSE P.M., INGARD K.U. (1968), *Theoretical Acoustics*, McGraw-Hill, New York.

15. ORTIZ S., GONZÁLEZ L.M., GONZÁLEZ DÍAZ C., SVENSSON U.P., COBO P. (2016), *Acoustic resonances in a 3D open cavity with non-parallel walls*, Journal of Sound and Vibration, **363**, 181–198.

16. PELAT A., FÉLIX S., PAGNEUX V. (2009), *On the use of leaky modes in open waveguides for the sound propagation modeling in street canyons*, The Journal of the Acoustical Society of America, **126**, 6, 2864–2872.

17. PRAKASH S., KUMAR T.G.R., RAJA S., DWARAKA-NATHAN D., SUBRAMANI H., KARTHIKEYAN C. (2016), *Active vibration control of a full scale aircraft wing using a reconfigurable controller*, Journal of Sound and Vibration, **361**, 32–49.

18. RDZANEK W.P. (2016), *The acoustic power of a vibrating clamped circular plate revisited in the wide low frequency range using expansion into the radial polynomials*, The Journal of the Acoustical Society of America, **139**, 6, 3199–3213.

19. RDZANEK W.P., RDZANEK W.J., SZEMELA K. (2016), *Sound radiation of the resonator in the form of a vibrating circular plate embedded in the outlet of the circular cylindrical cavity*, Journal of Computational Acoustics, **24**, 1650018 (23 pages).

20. SNAKOWSKA A. (2008), *Diffraction of sound waves at the opening of a soft cylindrical duct*, European Physical Journal – S T, **154**, 1, 201–206.

21. SNAKOWSKA A., JURKIEWICZ J., GORAZD Ł. (2017), *A hybrid method for determination of the acoustic impedance of an unflanged cylindrical duct for multimode wave*, Journal of Sound and Vibration, **396**, 325–339.

22. SOMMERFELD A. (1964), *Partial Differential Equation in Physics, Lectures on Theoretical Physics*, Academic Press, New York.

23. SZEMELA K. (2015), *Sound radiation inside an acoustic canyon with a surface sound source located at the bottom*, Journal of Computational Acoustics, **23**, 1550014 (22 pages).

24. SZEMELA K. (2017), *The sound radiation from a surface source located at the bottom of an open rectangular cavity*, Acta Acustica united with Acustica, **103**, 2, 189–199.

25. TROIAN R., SHIMOYAMA K., GILLOT F., BESSET S. (2016), *Methodology for the design of the geometry of a cavity and its absorption coefficients as random design variables under vibroacoustic criteria*, Journal of Computational Acoustics, **24**, 1650006 (12 pages).

26. UNRUH O., SINAPIUS M., MONNER H.P. (2015), *Sound radiation properties of complex modes in rectangular plates: a numerical study*, Acta Acustica united with Acustica, **101**, 1, 62–72.

27. WICIAK J., TROJANOWSKI R. (2015), *Evaluation of the effect of a step change in piezo actuator structure on vibration reduction level in plates*, Archives of Acoustics, **40**, 1, 71–79.

28. WRONA S., PAWEŁCZYK M. (2016), *Feedforward control of a light-weight device casing for active noise reduction*, Archives of Acoustics, **41**, 3, 499–505.

29. YANG C., CHENG L. (2016), *Prediction of noise inside an acoustic cavity of elongated shape using statistical energy analyses with spatial decay consideration*, Applied Acoustics, **113**, 34–38.

30. ZAWIESKA W.M., RDZANEK W.P. (2007), *The influence of a vibrating rectangular piston on the acoustic power radiated by a rectangular plate*, Archives of Acoustics, **32**, 2, 405–415.